How to extract the oscillating components of a signal? A wavelet-based approach compared to the Empirical Mode Decomposition

Adrien DELIÈGE

University of Liège, Belgium

Liège, December 22, 2016

adrien.deliege@ulg.ac.be

- Decomposing time series into several modes has become more and more popular and useful in signal analysis.
- Methods such as EMD, SSA, STFT, EWT, wavelets,... have been successfully applied in medicine, finance, climatology, ...
- Old but gold: Fourier transform allows to decompose a signal as

$$f(t) \approx \sum_{k=1}^{J} c_k \cos(\omega_k t + \phi_k).$$

- Problem: often too many components in the decomposition.
- Idea: Considering the amplitudes and frequencies as functions of t to decrease the number of terms:

$$f(t) = \sum_{k=1}^{K} a_k(t) \cos(\phi_k(t))$$

  with $K \ll J$ (AM-FM signals).
- We will focus on the EMD and a wavelet-based method.

EMD

- Empirical Mode Decomposition
- Empirical $=$ no strong theoretical background
- Decomposes a signal into IMFs (Intrinsic Mode Functions)
- Is often used with the Hilbert-Huang transform to represent the IMFs in the TF plane (not shown here).

EMD

1) For a signal $X(t)$, let

$$m_{1,0}(t) = \frac{u_{1,0}(t) + l_{1,0}(t)}{2}$$

be the mean of its upper and lower envelopes $u(t)$ and $l(t)$ as determined from a cubic-spline interpolation of local maxima and minima.

2) Compute $h_{1,0}(t)$ as:

$$h_{1,0}(t) = X(t) - m_{1,0}(t).$$

3) Now $h_{1,0}(t)$ is treated as the data, $m_{1,1}(t)$ is the mean of its upper and lower envelopes, and the process is iterated (“sifting process”):

$$h_{1,1}(t) = h_{1,0}(t) - m_{1,1}(t).$$

4) The sifting process is repeated k times, i.e.

$$h_{1,k}(t) = h_{1,k-1}(t) - m_{1,k}(t),$$

until a stopping criterion is satisfied.

EMD

5) Then $h_{1,k}(t)$ is considered as the component $c_1(t)$ of the signal and the whole process is repeated with the rest

$$r_1(t) = X(t) - c_1(t)$$

instead of $X(t)$. Get $c_2(t)$ then repeat with $r_2(t) = r_1(t) - c_2(t)$, ...

By construction, the number of extrema is decreased when going from r_i to r_{i+1}, and the whole decomposition is guaranteed to be completed with a finite number of modes.

Stopping criterion for the sifting process: When computing $m_{i,j}(t)$, also compute

$$a_{i,j}(t) = \frac{u_{i,j}(t) - l_{i,j}(t)}{2} \quad \sigma_{i,j}(t) = \left| \frac{m_{i,j}(t)}{a_{i,j}(t)} \right|.$$

The sifting is iterated until $\sigma(t) < 0.05$ for 95% of the total length of $X(t)$ and $\sigma(t) < 0.5$ for the remaining 5%.

EMD - Illustration

Show time!

Continuous wavelet transform

Given a wavelet ψ and a function f, the wavelet transform of f at time t and at scale $a > 0$ is defined as

$$W_f(t,a) = \int f(x)\bar{\psi}\left(\frac{x-t}{a}\right)\frac{dx}{a}$$

where $\bar{\psi}$ is the complex conjugate of ψ.
We use the wavelet ψ defined by its Fourier transform as

$$\hat{\psi}(\nu) = \sin\left(\frac{\pi\nu}{2\Omega}\right) e^{\frac{-(\nu-\Omega)^2}{2}}$$

with $\Omega = \pi\sqrt{2/\ln 2}$, which is similar to the Morlet wavelet but with exactly one vanishing moment.

CWT

Real and Imaginary parts of ψ

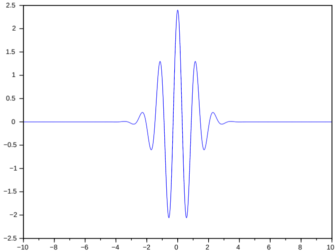

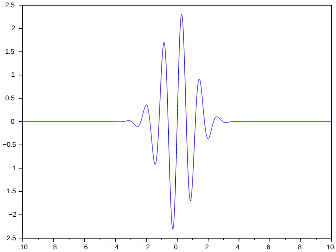

CWT

Real and Imaginary parts of ψ compared to a cosine.

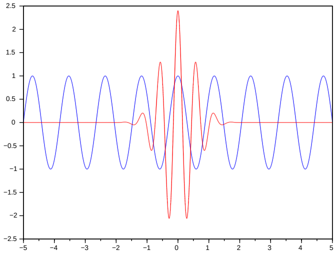

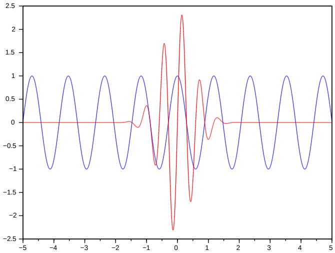

$\Re(W_f(0,a)) \approx 0$, $\Im(W_f(0,a)) \approx 0$ thus $|W_f(0,a)| \approx 0$.

CWT

Real and Imaginary parts of ψ compared to a cosine.

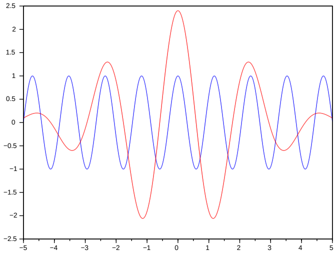

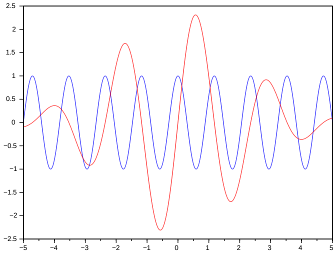

$\Re(W_f(0,a)) \approx 0$, $\Im(W_f(0,a)) \approx 0$ thus $|W_f(0,a)| \approx 0$.

CWT

Real and Imaginary parts of ψ compared to a cosine.

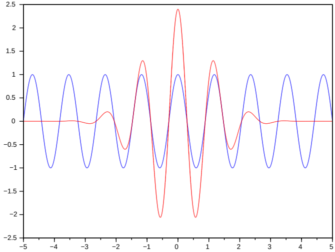

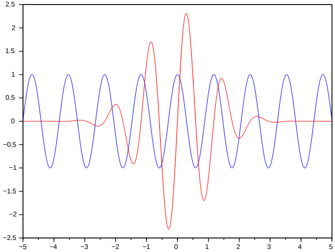

$\Re(W_f(0,a)) \approx 1$, $\Im(W_f(0,a)) \approx 0$ thus $|W_f(0,a)| \approx 1$.

CWT

Real and Imaginary parts of ψ compared to a cosine shifted.

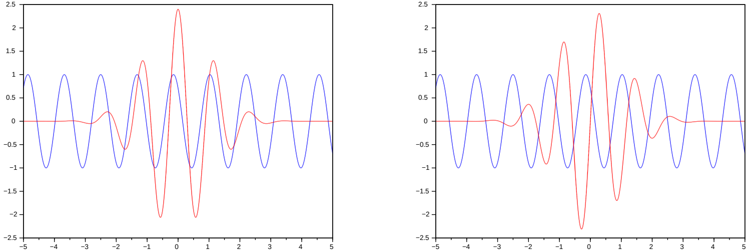

$\Re(W_f(0,a)) \approx \sqrt{2}/2$, $\Im(W_f(0,a)) \approx -\sqrt{2}/2$ thus $|W_f(0,a)| \approx 1$.

CWT

One has

$$|\hat{\psi}(\nu)| < 10^{-5} \text{ if } \nu \leq 0$$

thus ψ can be considered as a progressive wavelet (i.e. $\hat{\psi}(\nu) = 0$ if $\nu \leq 0$).

Property: If $f(x) = \cos(\omega x)$, then

$$W_f(t,a) = \frac{1}{2} e^{it\omega} \overline{\hat{\psi}(a\omega)}.$$

Consequence: Given t, if a^* is the scale at which

$$a \mapsto |W_f(t,a)|$$

reaches its maximum, then

$$a^* \omega = \Omega.$$

The value of ω can be obtained (if unknown) and f is recovered as

$$f(x) = 2\Re(W_f(x,a^*)) = 2|W_f(x,a^*(x))| \cos(\arg W_f(x,a^*(x))).$$

CWT

$$f(x) = \cos\left(\frac{2\pi}{32}x\right)$$

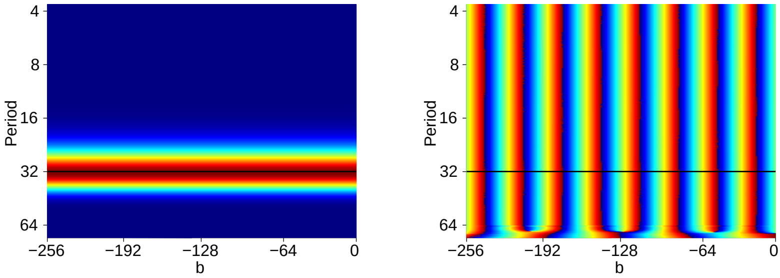

Left: $\left|W_f(t,a)\right|$. Right: $\arg(W_f(t,a))$.

CWT

$$f(x) = \cos\left(\frac{2\pi}{32}x\right)$$

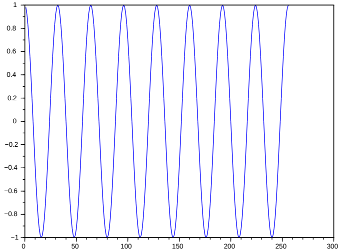

Left: initial signal. Right: Reconstructed signal superimposed to initial signal. Difference of order 10^{-5}.

CWT

What to do with this?

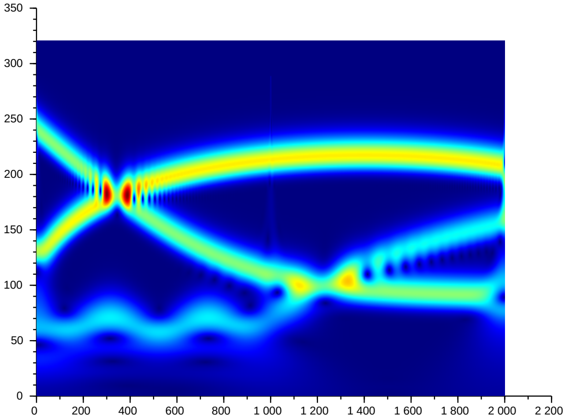

WIME - Wavelet-Induced Mode Extraction

1) Perform the CWT of the signal f: $W_f(t,a)$.
2) Compute the wavelet spectrum Λ associated to f:

$$a \mapsto \Lambda(a) = E_t \left|W_f(t,a)\right|$$

   where E_t denotes the mean over time.
3) Segment the spectrum to isolate the scale a^* at which Λ reaches its highest local maximum between the scales a_1 and a_2 at which Λ displays the left and right local minima that are the closest to a^*. We set $A = [a_1, a_2]$.
4) Choose a starting point $(t_0, a(t_0))$ with $a(t_0) \in A$, e.g.

$$(t_0, a(t_0)) = \underset{t,\ a \in A}{\operatorname{argmax}} \left|W_f(t,a)\right|.$$

WIME

5) Compute the ridge $t \mapsto (t, a(t))$ forward and backward that stems from $(t_0, a(t_0))$:
   a) Compute b_1 and b_2 such that $b_2 - b_1 = a_2 - a_1$ and $a(t_0) = (b_1 + b_2)/2$, i.e. center $a(t_0)$ in a frequency band of the same length as the initial one.
   b) Among the scales at which the function $a \mapsto |W_f(t_0 + 1, a)|$ ($a \in [b_1, b_2]$) reaches a local maximum, define $a(t_0 + 1)$ as the closest one to $a(t_0)$. If there is no local maximum, then $a(t_0 + 1) = b_1$ if $|W_f(t_0 + 1, b_1)| > |W_f(t_0 + 1, b_2)|$, and $a(t_0 + 1) = b_2$ otherwise.
   c) Repeat step 5) with $(t_0 + 1, a(t_0 + 1))$ instead of $(t_0, a(t_0))$ until the end of the signal.
   d) Proceed in the same way backward from $(t_0, a(t_0))$ until the beginning of the signal.

6) Extract the component associated to the ridge:

$$t \mapsto 2\Re(W_f(t, a(t))) = 2|W_f(t, a(t))| \cos(\arg W_f(t, a(t))).$$

WIME

7) That component is c_1. The whole process is repeated with the rest

$$r_1 = f - c_1$$

instead of f. Get c_2 then repeat with $r_2(t) = r_1(t) - c_2(t)$, ...

8) Stop the process when the extracted components are not relevant anymore, e.g. at c_n if $||c_n|| < 0.05 \max_{j<n} ||c_j||$.

Alternative stopping criterion : EMD-like method e.g. $|c_n| < 0.05 \max_{j<n} |c_j|$ for 95% of the duration and $|c_n| < 0.5 \max_{j<n} |c_j|$ for the remaining 5%.

Very useful: $(t,a) \mapsto |W_f(t,a)|$ can be seen as a TF representation of f.

WIME - Illustration

Show time again!

WIME - Illustration

We consider the function $f = f_1 + f_2$ defined on $[0,1]$ by

$$f_1(t) = \begin{cases} \cos(60\pi t) & \text{if } t \leq 0.5 \\ \cos(80\pi t - 15\pi) & \text{if } t > 0.5 \end{cases}$$

$$f_2(t) = \cos(10\pi t + 10\pi t^2).$$

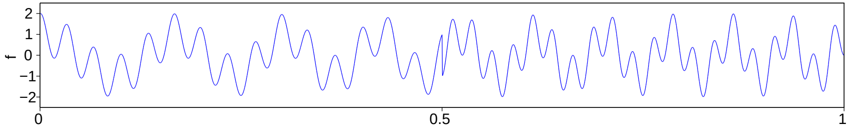

WIME - Illustration

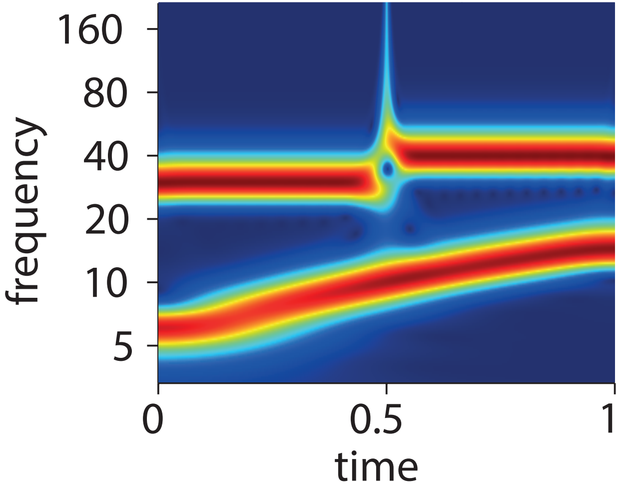

Time-frequency representation of f: $(t,a) \mapsto |W_f(t,a)|$.

WIME - Illustration

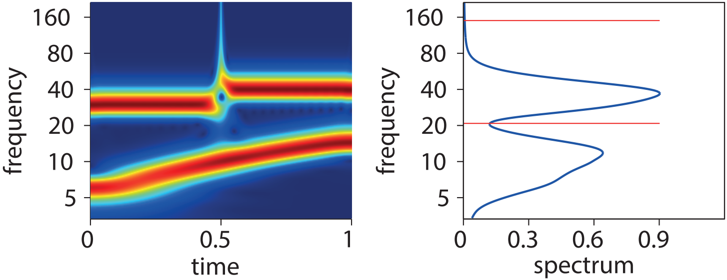

Time-frequency representation of f and spectrum $a \mapsto \Lambda(a) = E_t\, |W_f(t, a)|$.

WIME - Illustration

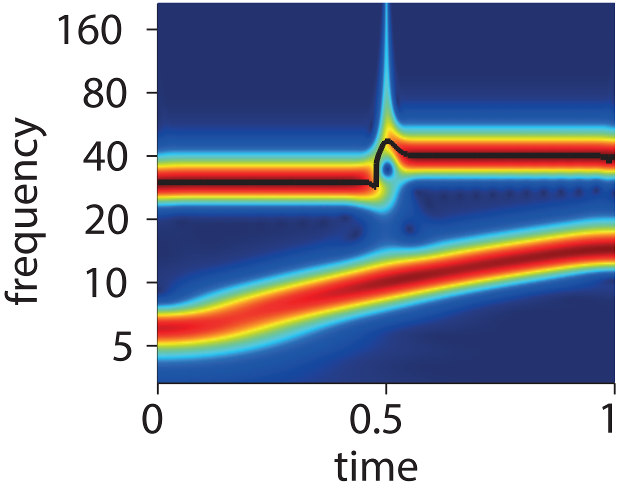

First ridge.

WIME - Illustration

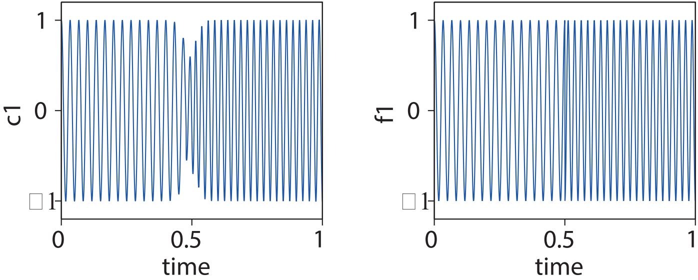

First component c_1 extracted and expected component f_1.

WIME - Illustration

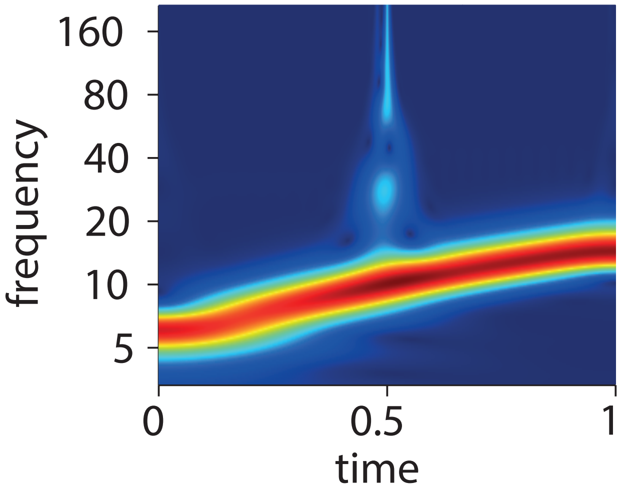

Time-frequency representation of $r_1 = f - c_1$.

WIME - Illustration

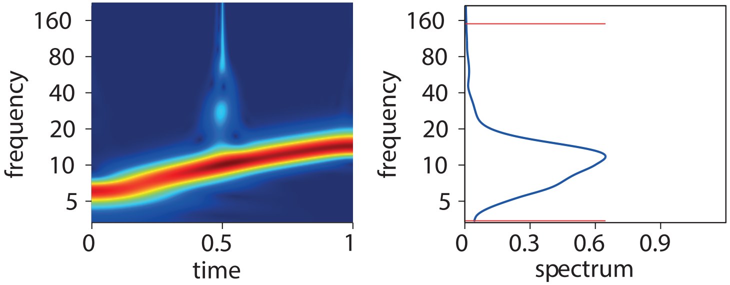

Time-frequency representation of $r_1 = f - c_1$ and spectrum.

WIME - Illustration

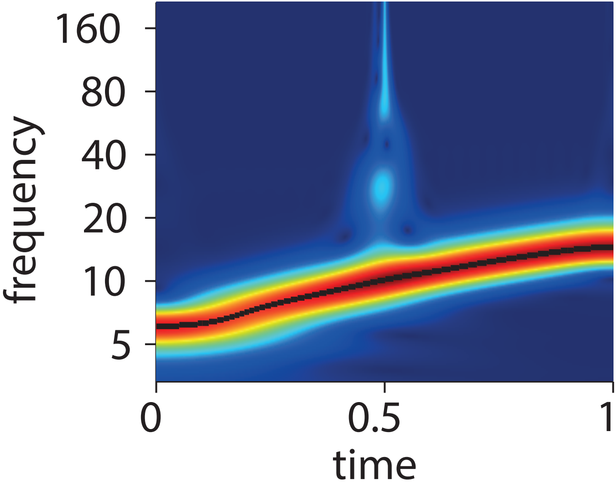

First ridge.

WIME - Illustration

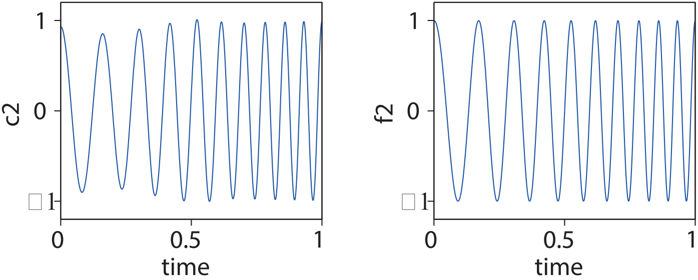

Second component c_2 extracted and expected component $r_1 = f - c_1$.

WIME - Illustration

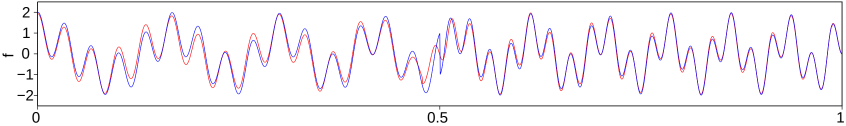

Original and reconstructed signal.

WIME - Illustration

With an AM-FM signal

$$f_1(t) = (2+\sin(5\pi t))\cos(100(t-0.5)^3+100t)$$
$$f_2(t) = \begin{cases} (1.5+t)\cos(0.2e^{10t}+350t) & \text{if } t \leq 0.5 \\ t^{-1}\cos(-300t^2+1000t) & \text{if } t > 0.5 \end{cases}$$

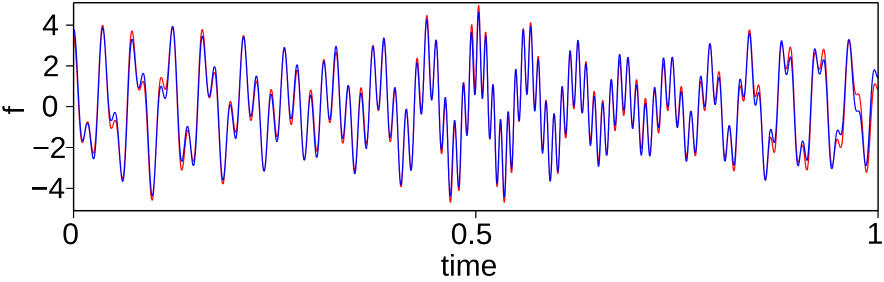

WIME - Illustration

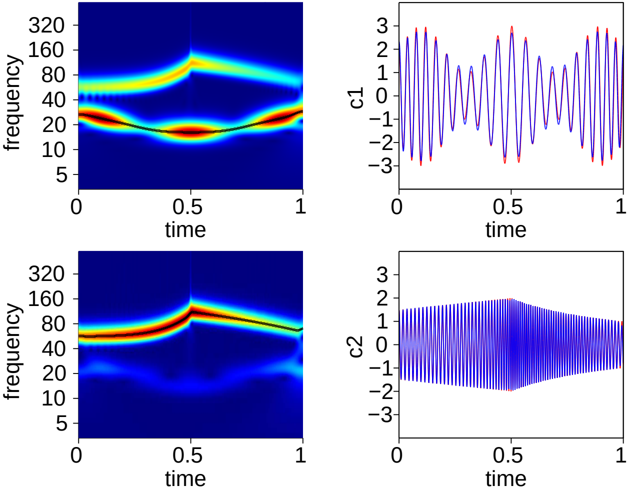

EMD vs WIME

Round 1
Crossings in the TF plane

EMD vs WIME: Crossings in the TF plane

We consider $f = f_1 + f_2 + f_3$ (on $[0,1]$) made of three FM-components with constant amplitudes of 1.25, 1, 0.75:

$$f_1(t) = 1.25\cos((10t-7)^3 - 1800t)$$

$$f_2(t) = \cos(360(0.5)^{10t} - 200t)$$

$$f_3(t) = \begin{cases} 0.75\cos(125t + \cos(30t)) & \text{if } t \leq 0.5 \\ 0.75\cos(-500t^2 + 375t) & \text{if } t > 0.5 \end{cases}$$

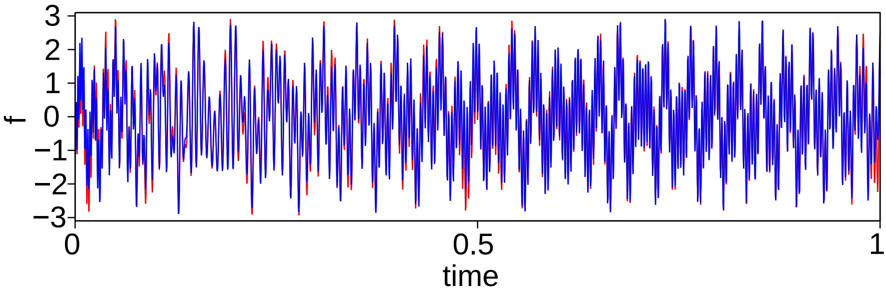

EMD vs WIME: Crossings in the TF plane - WIME

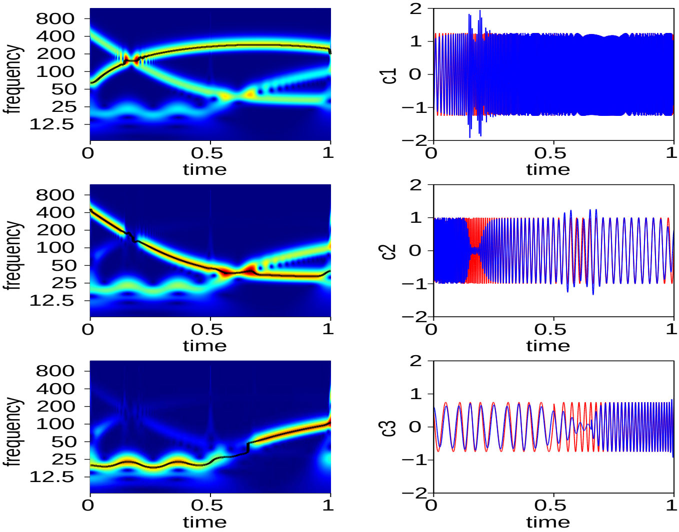

EMD vs WIME: Crossings in the TF plane - EMD

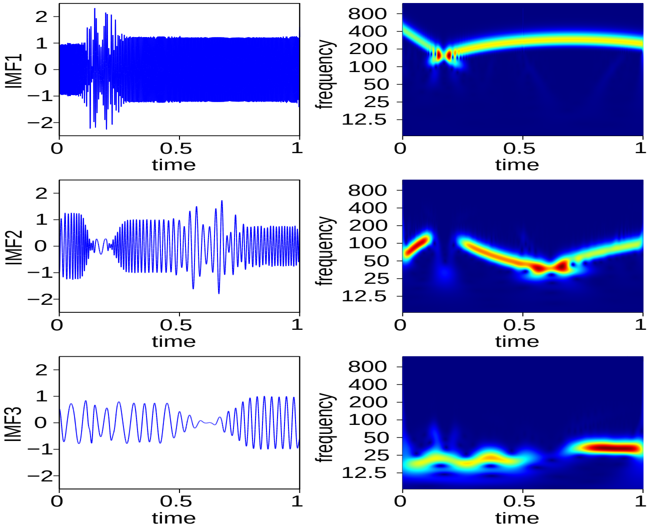

EMD vs WIME: Crossings in the TF plane - WIME-EMD

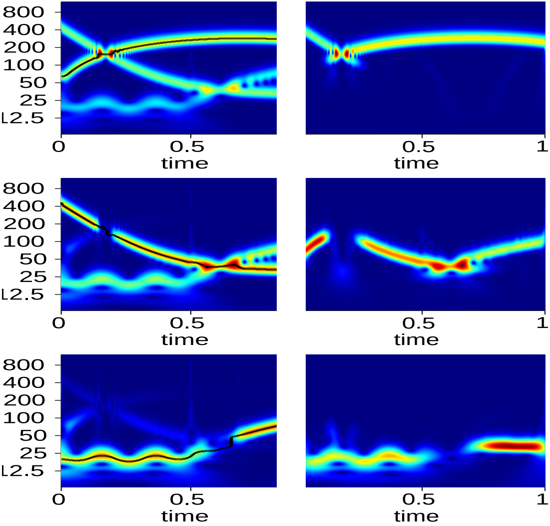

EMD vs WIME: Crossings in the TF plane

- The influence of the crossings between the patterns in the TF plane remains limited for WIME.
- The energy-based hierarchy among the components is respected for WIME
- The EMD follows an "upper ridge first" scheme and can't proceed otherwise.

EMD vs WIME

Round 2

Mode-mixing problem

EMD vs WIME: Mode-mixing problem

We consider a signal made of AM-FM components that are not “well-separated” with respect to their frequency nor with their amplitudes. Objective: recover the original frequencies used to build the signal. We consider $f = \sum_i f_i$ with

$$
\begin{aligned}
f_1(t) &= \left(1 + 0.5\cos\left(\frac{2\pi}{200}t\right)\right)\cos\left(\frac{2\pi}{47}t\right)\\
f_2(t) &= \frac{\ln(t)}{14}\cos\left(\frac{2\pi}{31}t\right)\\
f_3(t) &= \frac{\sqrt{t}}{60}\cos\left(\frac{2\pi}{65}t\right)\\
f_4(t) &= \frac{t}{2000}\cos\left(\frac{2\pi}{23+\cos\left(\frac{2\pi}{1600}t\right)}t\right).
\end{aligned}
$$

Target frequencies: 1/47, 1/31, 1/65, and $\approx$ 1/23 Hz. Note that t takes integer values from 1 to 800.

EMD vs WIME: Mode-mixing problem

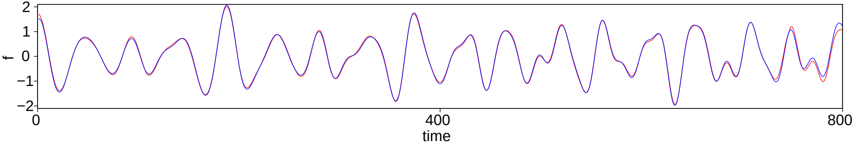

Target frequencies: 1/47, 1/31, 1/65, and $\approx$ 1/23 Hz.

EMD vs WIME: Mode-mixing problem - WIME

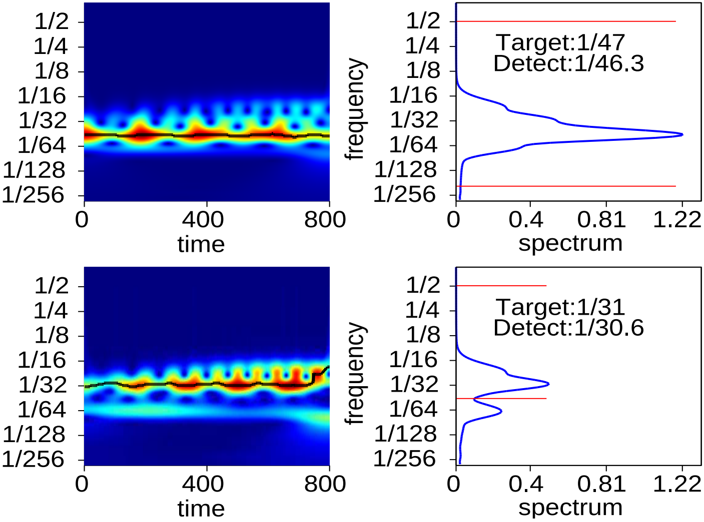

EMD vs WIME: Mode-mixing problem - WIME

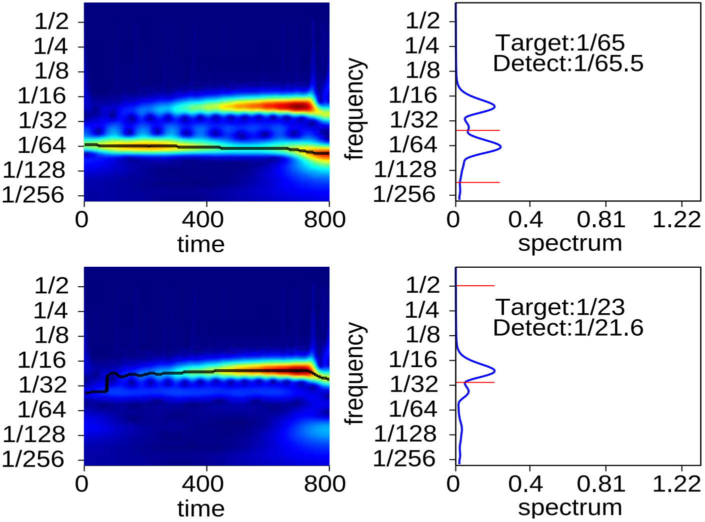

EMD vs WIME: Mode-mixing problem - WIME

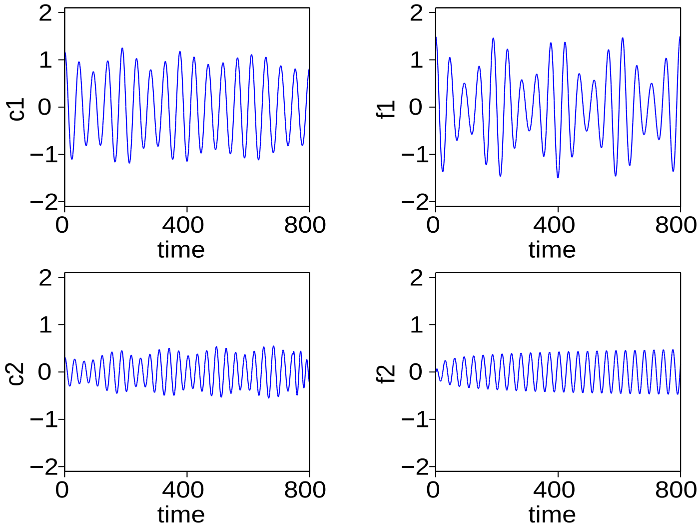

EMD vs WIME: Mode-mixing problem - WIME

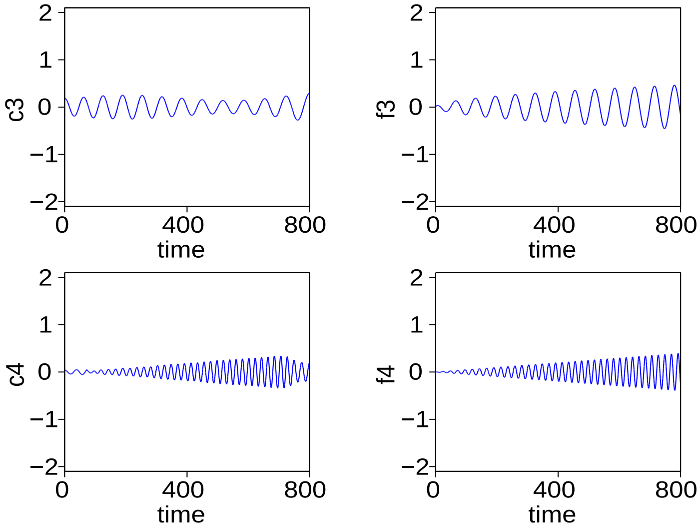

EMD vs WIME: Mode-mixing problem - EMD

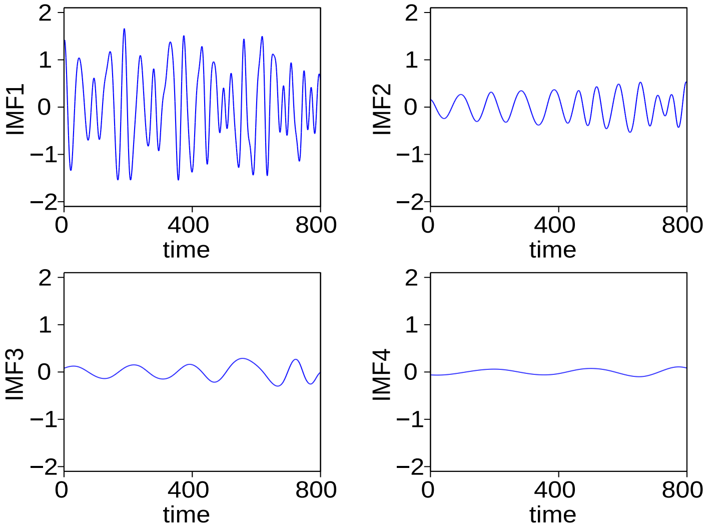

EMD vs WIME: Mode-mixing problem - WIME - EMD

Target	WIME	EMD
1/23	1/21.6	-
1/31	1/30.6	-
1/47	1/46.3	1/41
1/65	1/65.5	1/75
-	-	1/165
-	-	1/284

- IMF1 is almost the signal itself - correlation of 0.93.
- EMD cannot resolve the mode-mixing problem.
- WIME provides accurate information.

EMD vs WIME

Round 3

Resistance to noise

Resistance to noise

We consider the chirp f defined on $[0,1]$ by

$$f(t) = \cos(70t + 30t^2)$$

and a Gaussian white noise X of zero mean and variance 1 and we run WIME on f, $f + X$, $f + 2X$ and $f + 3X$.

Resistance to noise: WIME

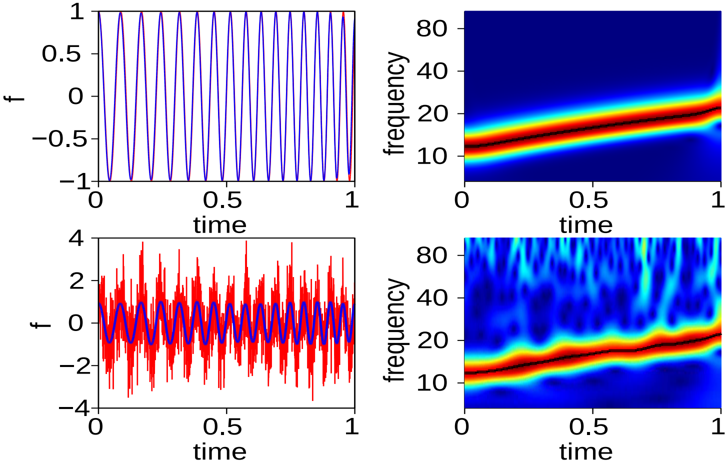

WIME with f and $f+X$.

Resistance to noise: WIME

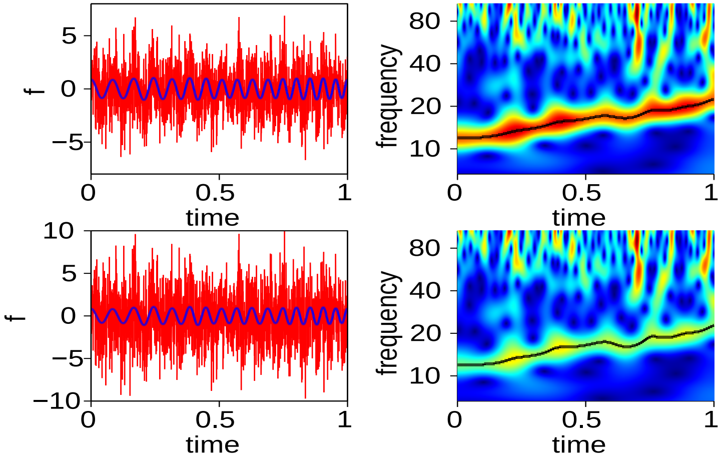

WIME with $f + 2X$ and $f + 3X$.

Resistance to noise: EMD

Not performed since:

- It is known (and obvious) that EMD is not noise-resistant.
- It first gives many noisy IMFS.
- It is not fair to compare EMD with WIME; improved versions of the EMD should be used instead, e.g. Ensemble Empirical Mode Decomposition (EEMD) and Complete Ensemble Empirical Mode Decomposition with Adaptive Noise (CEEMDAN).
- Improvements of EMD are made to the detriment of computational costs.
- WIME is naturally resistant and the scales to use for the reconstruction can be selected.

Real-life example: ECG

Real-life example
Electrocardiogram

Real-life example: ECG

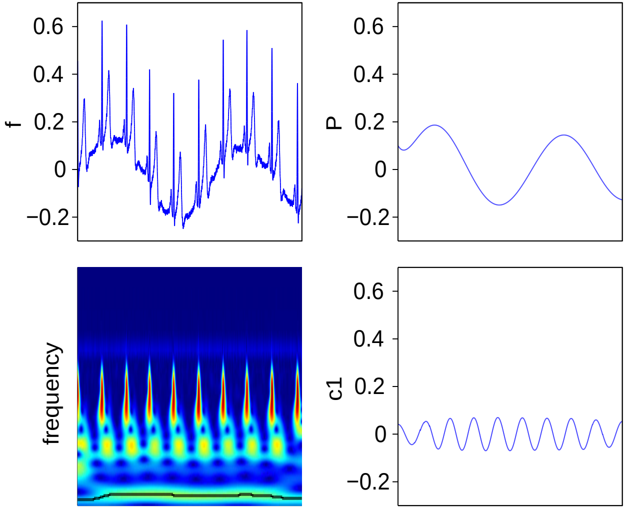

Real-life example: ECG

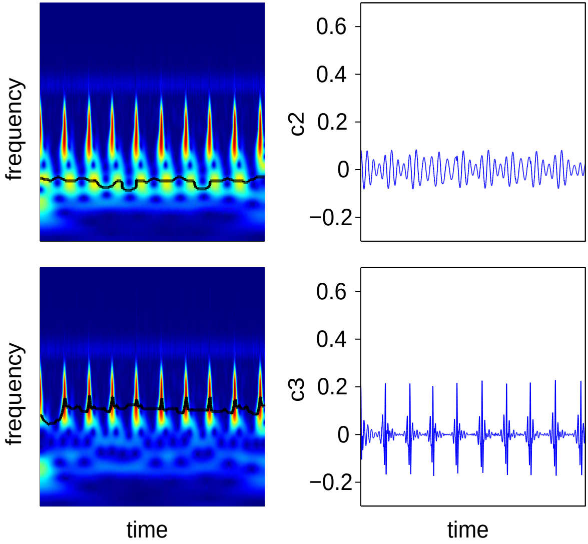

Real-life example: ECG

- The Dirac-like impulses make it an approximation of an AM-FM signal.
- WIME extracts valuable information.
- It decomposes the signal into simpler components easy to analyze.
- It could be useful to compare hundreds of patients.
- EMD provides 14 IMFS, many of them are noisy.

EMD vs WIME: Some conclusions

- EMD is fully data-driven but sensitive to noise and not flexible (black box).
- EMD extract components before visualizing them.
- EMD follows “upper ridge first” principle, thus have problems with intersecting frequencies and mode mixing.
- EMD has codes available on the internet.
- ...
- WIME is flexible but works in the frequency domain. Visualization prior to the analysis allows more freedom.
- WIME respects the hierarchical structure imposed by the energy of the components thus have better skills when EMD is in trouble.
- WIME is naturally tolerant to noise.
- WIME can provide a finer analysis of the data.
- ...

Edge effects

What you often see in practice

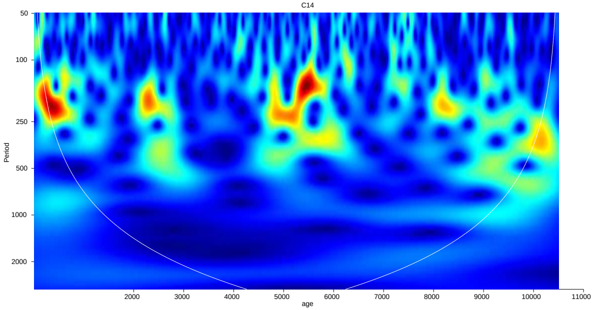

Edge effects

In practice: the signal has to be padded at its edges to obtain the CWT.
Possibilities:

- zero-padding
- orthogonal symmetry (mirroring)
- central symmetry (inverse mirroring)
- periodization

If possible, the padding needs to have the same properties as the signal.
Zero-padding: “universality”, independent of the signal.

Zero-padding

Expected: $W_f(t,\Omega/\omega) = \frac{1}{2}e^{it\omega}$ thus $|W_f(t,\Omega/\omega)| = 0.5$.
What happens with a simple cosine:

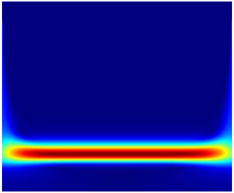

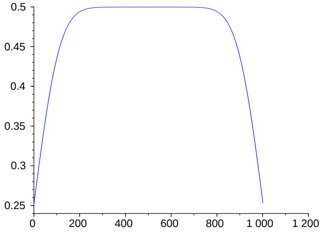

Ridge : straight line.
The amplitude decreases at the borders. The instantaneous frequency increases at the end (not shown). This confirms intuition.

Zero-padding

Expected: $W_f(t,\Omega/\omega) = \frac{1}{2}e^{it\omega}$ thus $|W_f(t,\Omega/\omega)| = 0.5$.
What happens with a simple cosine $f(x) = \cos(2\pi/100x)$:

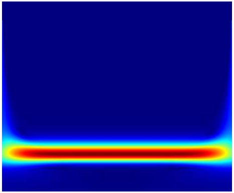

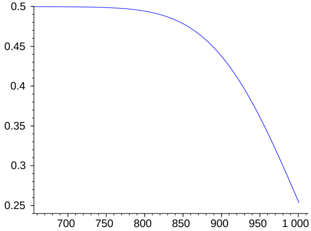

Ridge : straight line.
The amplitude decreases at the borders. The instantaneous frequency increases at the end (not shown). This confirms intuition.

Zero-padding

Expected: $W_f(t, \Omega/\omega) = \frac{1}{2}e^{it\omega}$ thus $|W_f(t, \Omega/\omega)| = 0.5$.
What happens with a simple cosine $f(x) = \cos(2\pi/100x)$:

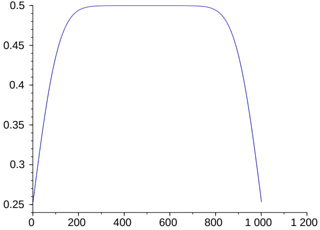

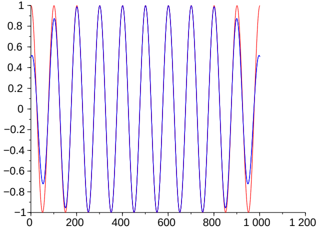

Ridge : straight line.
The amplitude decreases at the borders. The instantaneous frequency increases at the end (not shown). This confirms intuition.

Zero-padding: In theory

This is due to the finite length of the signal. Mathematically, in this case,

$$f(x) = \cos(\omega x)\chi_{]-\infty,0]}(x)$$

and thus for $a = \Omega/\omega$,

$$W_f(t,\Omega/\omega) = \frac{1}{2}e^{it\omega}z(t)$$

with

$$\Re(z(t)) = \frac{1}{2} - \frac{2}{\pi}\int_0^1 \frac{\overline{\hat{\psi}(\Omega x)}(x^2-2x-1)}{(x^2-1)(3-x)}\sin(t\omega(1-x))dx$$

and

$$\Im(z(t)) = \frac{2}{\pi}\int_0^1 \frac{\overline{\hat{\psi}(\Omega x)}}{(x+1)(3-x)}\cos(t\omega(1-x))dx.$$

Zero-padding: In theory

$W_f(t,\Omega/\omega) = \frac{1}{2}e^{it\omega}z(t)$, study of $z(t)$:

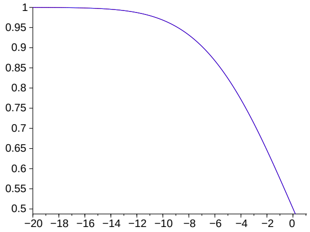

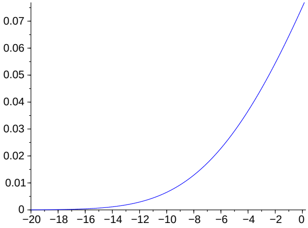

Amplitude and argument of z as function of t. These confirm intuition and experiments.

A possible solution? Iterations!

- The theoretical result is difficult to use in practice.
- All the energy has not be drained from the TF plane, there is still some energy left at the borders.
- Iterate the extraction process along the same ridge to sharpen the component before getting interested in another ridge.
- Stop iterations when the component extracted is not significant anymore, e.g. at iteration J if the extracted component at iteration J has less than 95% of the energy of the extracted component at the first extraction.

A possible solution? Iterations!

Iteration 1

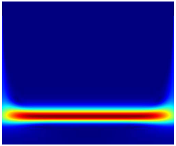

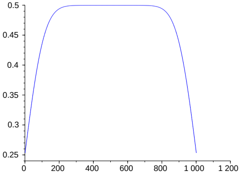

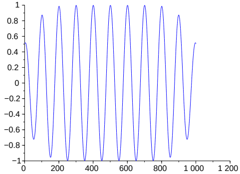

A possible solution? Iterations!

Iteration 2

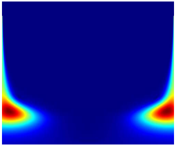

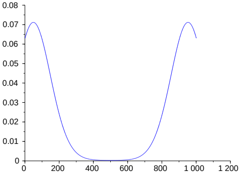

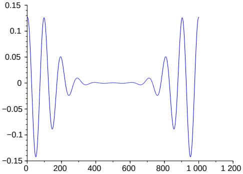

A possible solution? Iterations!

Iteration 3

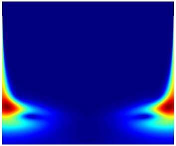

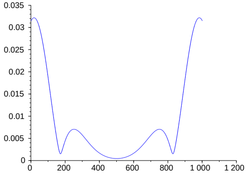

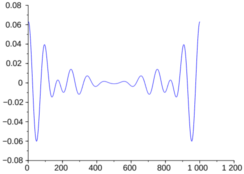

A possible solution? Iterations!

Iteration 4

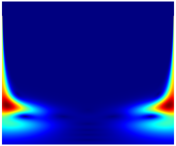

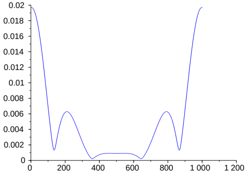

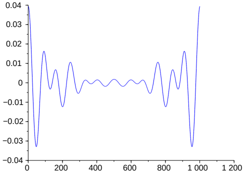

A possible solution? Iterations!

Iteration 5

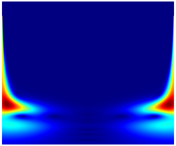

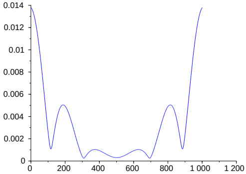

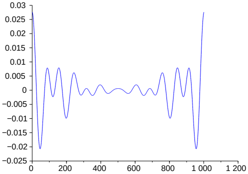

A possible solution? Iterations!

Iteration 50

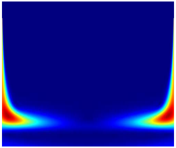

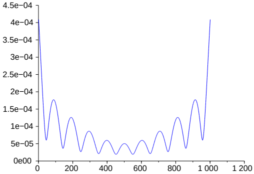

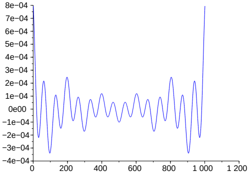

A possible solution? Iterations!

Iteration 1

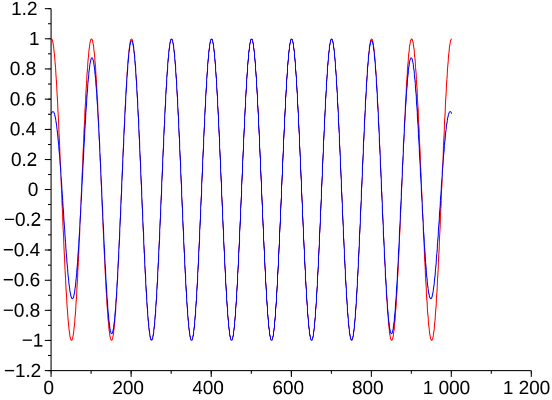

A possible solution? Iterations!

Iteration 2

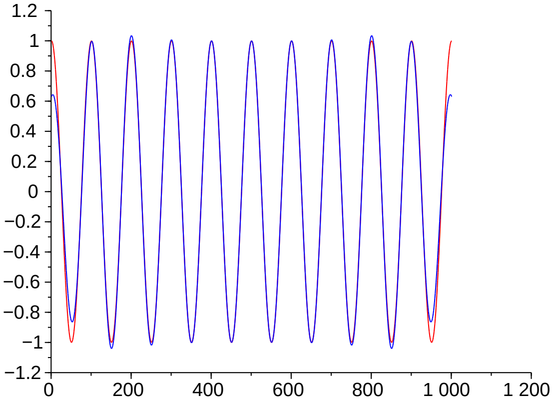

A possible solution? Iterations!

Iteration 3

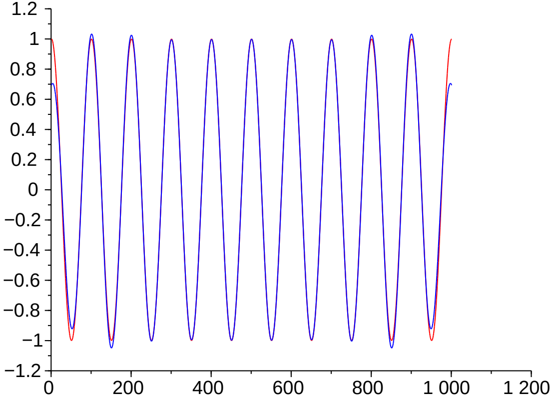

A possible solution? Iterations!

Iteration 4

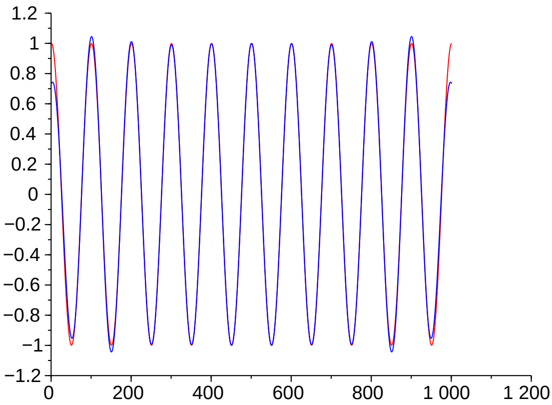

A possible solution? Iterations!

Iteration 5

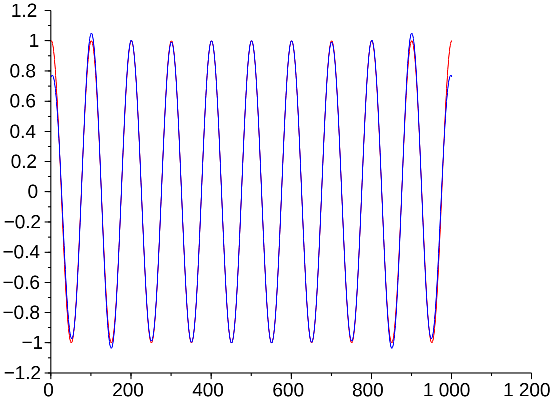

A possible solution? Iterations!

Iteration 10

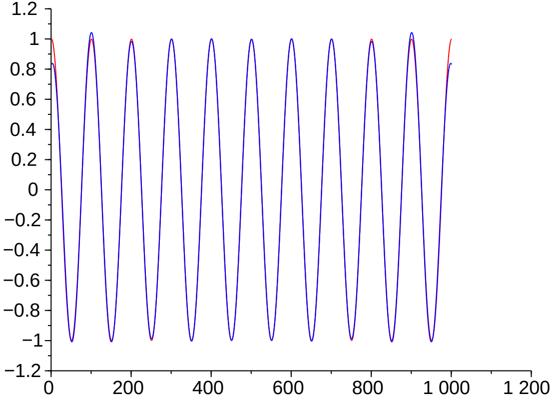

A possible solution? Iterations!

Iteration 20

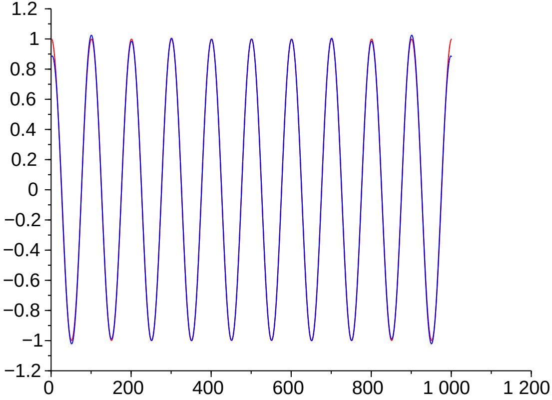

A possible solution? Iterations!

Iteration 50

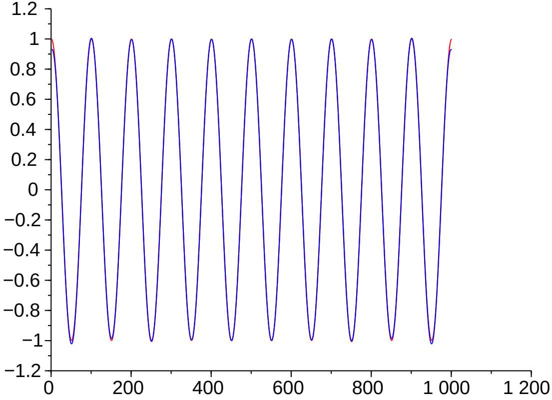

A possible solution? Iterations!

Iteration 100

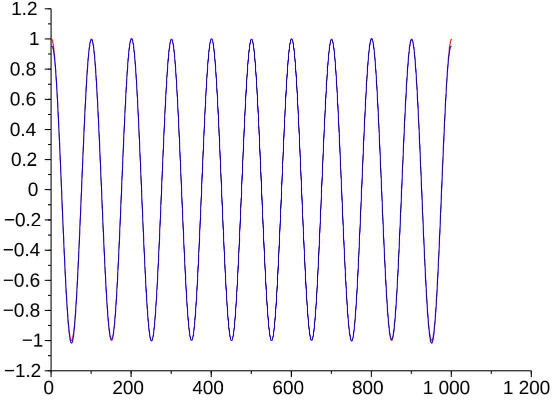

Some ideas

Perfect correction of border effects $\Rightarrow$ Terrific forecasts!

Idea: perform the CWT, extract dominant components (with corrected border effects), extrapolate the components (smooth AM-FM signals), then add the components to reconstruct and predict the signal.

Great idea. Doesn't work.

Instead: build a model based on the information provided by the CWT.

ENSO index

- Analyzed data: Niño 3.4 time series, i.e. monthly-sampled sea surface temperature anomalies in the Equatorial Pacific Ocean from Jan 1950 to Dec 2014 (`http://www.cpc.ncep.noaa.gov/`).

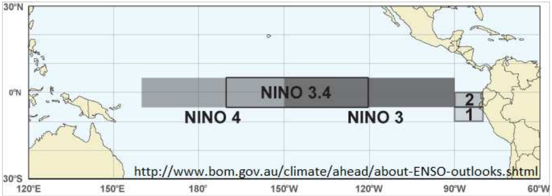

ENSO index

- Niño 3.4 index:

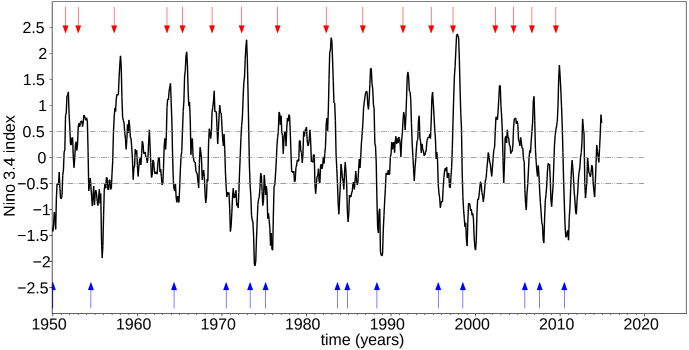

- 17 El Niño events: SST anomaly above $+0.5^\circ$C during 5 consecutive months.
- 14 La Niña events: SST anomaly below -0.5°C during 5 consecutive months.

ENSO index

- Flooding in the West coast of South America
- Droughts in Asia and Australia
- Fish kills or shifts in locations and types of fish, having economic impacts in Peru and Chile
- Impact on snowfalls and monsoons, drier/hotter/wetter/cooler than normal conditions
- Impact on hurricanes/typhoons occurrences
- Links with famines, increase in mosquito-borne diseases (malaria, dengue, ...), civil conflicts
- In Los Angeles, increase in the number of some species of mosquitoes (in 1997 notably).
- ...

Analysis

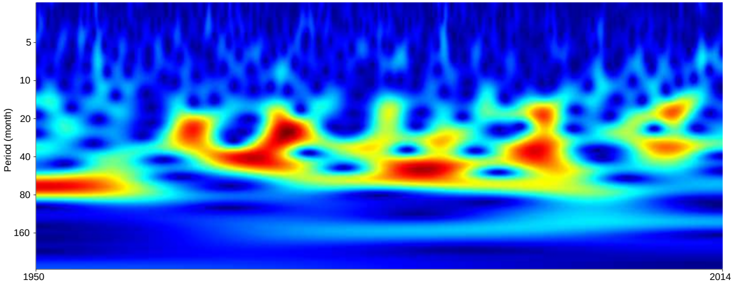

Analysis

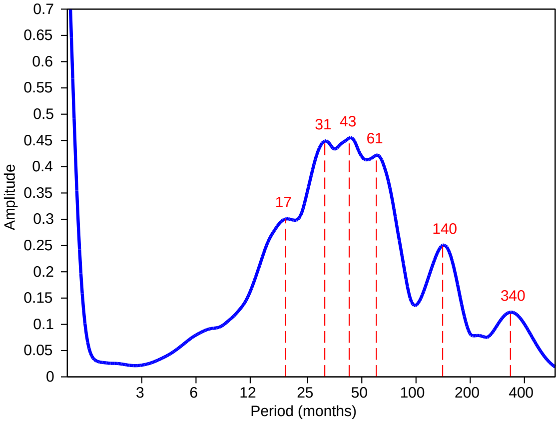

0.7
0.65
0.6
0.55
0.5
0.45
0.4
0.35
0.3
0.25
0.2
0.15
0.1
0.05
0
Amplitude
3
6
12
25
50
100
200
400
Period (months)
17
31
43
61
140
340

Analysis

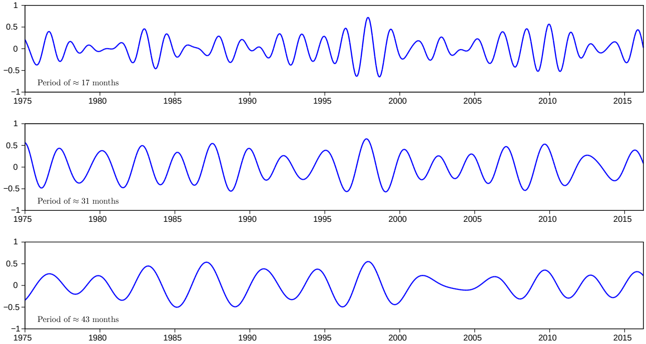
Period of ≈ 17 months
Period of ≈ 31 months
Period of ≈ 43 months
1975
1980
1985
1990
1995
2000
2005
2010
2015

Analysis

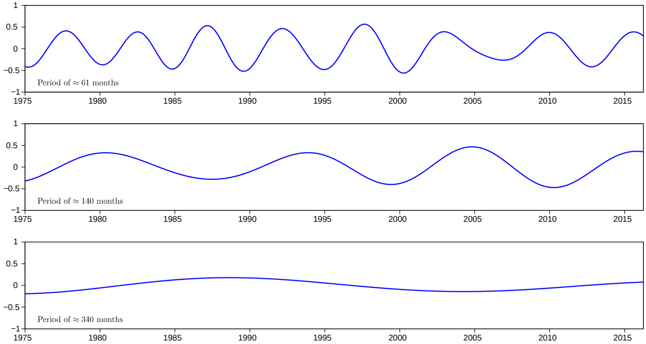
1
0.5
0
−0.5
−1
Period of ≈ 61 months
1975 1980 1985 1990 1995 2000 2005 2010 2015
1
0.5
0
−0.5
−1
Period of ≈ 140 months
1975 1980 1985 1990 1995 2000 2005 2010 2015
1
0.5
0
−0.5
−1
Period of ≈ 340 months
1975 1980 1985 1990 1995 2000 2005 2010 2015

Analysis

- Periods of $\approx 17, 31, 43, 61, 140$ months in agreement with previous studies.
- Period of $\approx$ 340 months can be an artifact; will be neglected.
- The low frequency components (corresponding to 31,43,61,140 months) capture $\approx$ 90$\%$ of the variability of the signal.
- These components appear relatively stationary thus easier to model.

Idea of the model

- Model the decadal oscillation and subtract it.
- Model a 61-months component phased with warm events and subtract it.
- Model a 31-months component phased with cold events and subtract it.
- Model a 43-months component phased with remaining warm and cold events.
- Extrapolate these modeled components and add them to obtain a forecast.

Model

Idea: build components that mimic the low-frequency ones and that are easy to extrapolate. Let us assume we have the signal up to time T (between 1995 and 2015).

1. Model the decadal oscillation. The amplitude A_{140} is estimated with the WS of s as 0.35 and we set

$$y_{140}(t) = A_{140}\cos(2\pi t/140 + 2.02).$$

2. We now work with $s_1 = s - y_{140}$. The WS of s_1 gives $A_{61} = 0.435$. Phase y_{61} with the strongest warm events of s_1, which occur approximately every 5 years: find the position p of the last local maximum of s_1 such that $s_1(p) > 0.5$. If $s_1(p) > 0.9$ then we set

$$y_{61}(t) = A_{61}\cos(2\pi(t-p)/61);$$

else

$$y_{61}(t) = -A_{61}\cos(2\pi(t-p)/61).$$

Model

3. We now work with $s_2 = s_1 - y_{61}$. The WS of s_2 gives $A_{31} = 0.42$. Phase y_{31} with the cold events of s_2, which occur approximately every 2.5 years. Find the position p of the last local minimum of s_2 such that $s_2(p) < -0.5$ and we set
$$y_{31}(t) = -A_{31}\cos(2\pi(t-p)/31).$$
4. We now work with $s_3 = s_2 - y_{31}$. The WS of s_3 gives $A_{43} = 0.485$. y_{43} has to explain the remaining warm and cold events of s_3. Find the position p of the last local maximum of s_3 such that $s_3(p) > 0.5$ and we set
$$y^1_{43}(t) = A_{43}\cos(2\pi(t-p)/43).$$
Then we find the position p of the last local minimum of s_3 such that $s_3(p) < -0.8$ and we set
$$y^2_{43}(t) = -A_{43}\cos(2\pi(t-p)/43).$$
Finally, we define
$$y_{43} = (y^1_{43} + y^2_{43})/2.$$

Model

5. Extend the signals $(y_i)_{i\in I}$ up to $T+N$ for N large enough (at least the number of data to be predicted). Then

$$y = \sum_{i\in I} y_i$$

stands for a first reconstruction (for $t \leq T$) and forecast (for $t > T$) of s.

6. We set $s(t) = y(t)$ for $t > T$, perform the CWT of s and extract the components $\hat{c}_j$ at scales j corresponding to 6, 12, 17, 31, 43, 61 and 140 months. These are considered as our final AM-FM components and $\hat{c} = \sum_j \hat{c}_j$ both reconstructs (for $t \leq T$) and forecasts (for $t > T$) the initial ONI signal in a smooth and natural way.

Skills of the model

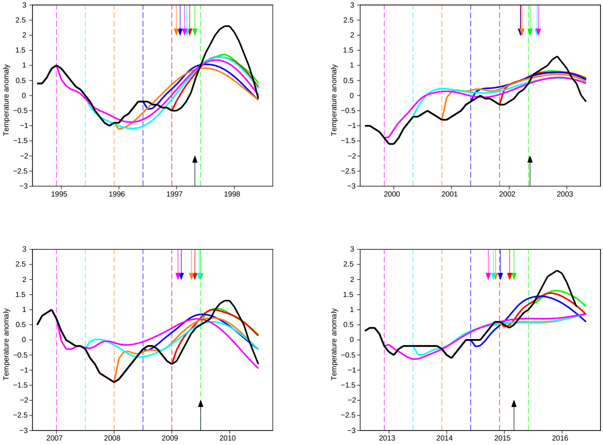

Skills of the model

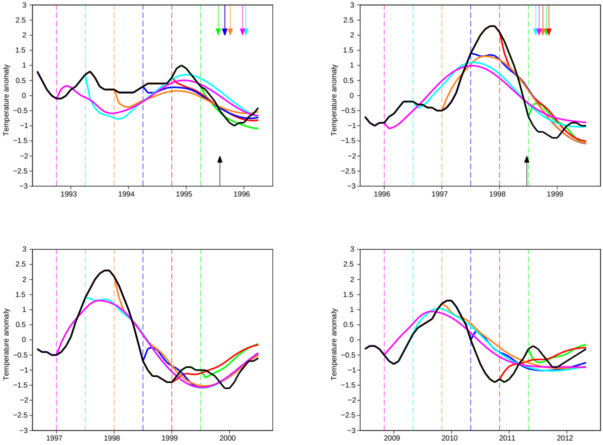

Skills of the model

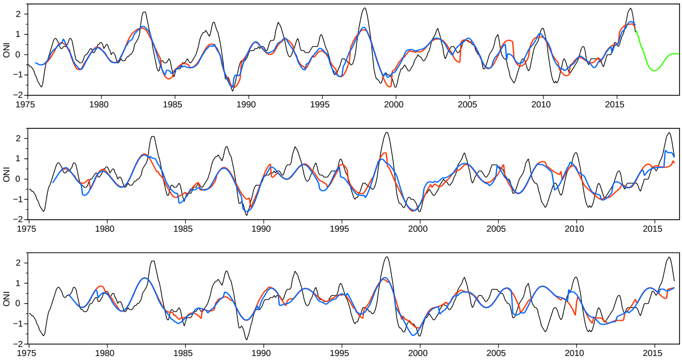

Skills of the model

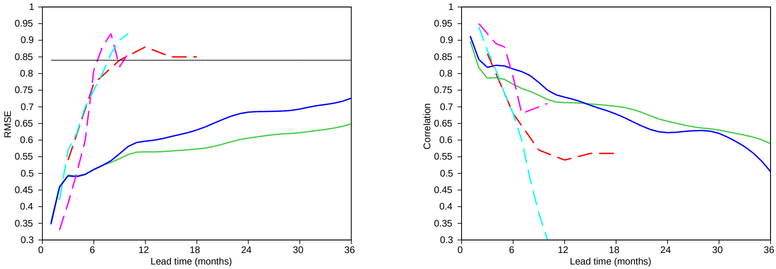

(slightly unfair) comparison with other works.

Some conclusions

- The periods detected are in agreement with previous works
- The information provided by the CWT allows to build a model for long-term forecasting
- Early signs of major EN and LN events can be detected 2-3 years in advance
- The ideas could be combined with other models that are better for short-term predictions
- We could improve the model with seasonal and annual variations
- We could make the amplitudes vary through time
- The important feature is the phase-locking of the components

Some references

EMD: [4, 5, 9, 11, 12] and
`http://perso.ens-lyon.fr/patrick.flandrin/emd.html`

CWT: [1, 2, 6, 7, 10]

WIME: [3, 8] + coming soon

Thank you

Thank you
for your attention

I. Daubechies.
Ten Lectures on Wavelets.
SIAM, 1992.

I. Daubechies, J. Lu, and H.-T. Wu.
Synchrosqueezed wavelet transforms: An empirical mode decomposition-like tool.
Journal of Applied and Computational Harmonic Analysis, 30(2):243–261, 2011.

A. Deliège and S. Nicolay.
A new wavelet-based mode decomposition for oscillating signals and comparison with the empirical mode decomposition.
In *Springer Proceedings of the 13th International Conference on Information Technology : New Generations, Las Vegas (NV), USA*, 2016.

P. Flandrin, G. Rilling, and P. Goncalves.
Empirical mode decomposition as a filter bank.
IEEE Signal Processing Letters, 11(2):112–114, 2004.

N. E. Huang, Z. Shen, S. R. Long, M. C. Wu, H. H. Shih, Q. Zheng, N.-C. Yen, C. C. Tung, and H. H. Liu.
The empirical mode decomposition and the Hilbert spectrum for nonlinear and non-stationary time series analysis.
Proceedings of the Royal Society of London A, 454:903–995, 1998.

S. Mallat.
A Wavelet Tour of Signal Processing.
Academic Press, 1999.

Y. Meyer and D. Salinger.
Wavelets and Operators, volume 1.
Cambridge university press, 1995.

S. Nicolay.
A wavelet-based mode decomposition.
European Physical Journal B, 80:223–232, 2011.

G. Rilling, P. Flandrin, and P. Goncalves.
On empirical mode decomposition and its algorithms.
In *IEEE-EURASIP Workshop Nonlinear Signal Image Processing (NSIP)*, 2003.

C. Torrence and G. Compo.
A practical guide to wavelet analysis.
Bulletin of the American Meteorological Society, 79:61–78, 1998.

M. E. Torres, M. A. Colominas, G. Schlotthauer, and P. Flandrin.
A complete ensemble empirical mode decomposition with adaptive noise.
In *IEEE International Conference on Acoustic, Speech and Signal Processing (ICASSP)*, 2011.

Z. Wu and N. E. Huang.
Ensemble empirical mode decomposition: a noise-assisted data analysis method.
Advances in Adaptative Data Analysis, 1:1–41, 2009.